Journal of Power Sources 267 (2014) 874–880

Contents lists available at ScienceDirect

Journal of Power Sources

journal homepage: www.elsevier.com/locate/jpowsour

Excellent high rate capability and high voltage cycling stability of Y_2O_3-coated $LiNi_{0.5}Co_{0.2}Mn_{0.3}O_2$

Xue-Hui Liu [a], Li-Qin Kou [a], Ting Shi [a], Kun Liu [a], Li Chen [a, b, *]

[a] Department of Chemistry, School of Science, Tianjin University, People's Republic of China
[b] Synergetic Innovation Center of Chemical Science and Engineering (Tianjin), Tianjin 300072, People's Republic of China

HIGHLIGHTS

- Electrochemical performance of $LiNi_{0.5}Co_{0.2}Mn_{0.3}O_2$ is improved by Y_2O_3 coating.
- Y_2O_3-coated samples show excellent high rate capability (10C and 20C).
- Good cycling stability at 10C under high voltages (4.6 V and 4.8 V) can be obtained.
- Y_2O_3 layer facilitates the diffusion of Li^+ at the electrode/electrolyte interface.

ARTICLE INFO

Article history:
Received 28 January 2014
Received in revised form
10 May 2014
Accepted 12 May 2014
Available online 20 May 2014

Keywords:
$LiNi_{0.5}Co_{0.2}Mn_{0.3}O_2$
Y_2O_3 coating
High rate
Cycling life
High cut-off voltage

ABSTRACT

Y_2O_3-coated $LiNi_{0.5}Co_{0.2}Mn_{0.3}O_2$ cathode materials show excellent cycling stability and higher rate capability than the bare $LiNi_{0.5}Co_{0.2}Mn_{0.3}O_2$ at higher cut-off voltages of 4.6 V and 4.8 V. The thickness of Y_2O_3-coating layer is about 5–15 nm, and the original structure of the $LiNi_{0.5}Co_{0.2}Mn_{0.3}O_2$ isn't influenced by Y_2O_3 coating layer. The 2 wt% Y_2O_3-coated $LiNi_{0.5}Co_{0.2}Mn_{0.3}O_2$ can deliver 114.5 mAh g^{-1} (76.3% of its initial discharge capacity) after 100 cycles at 10C (1800 mA g^{-1}) between 2.8 and 4.6 V, while the bare $LiNi_{0.5}Co_{0.2}Mn_{0.3}O_2$ delivers only 11.5 mAh g^{-1} with 8.3% capacity retention left. When the high cut-off voltage increases to 4.8 V, the capacity retention of 2 wt% Y_2O_3-coated sample is 49.0%, which is much higher than that of the bare sample (5.9%) at 10C after 100 cycles. The rate capabilities of 2 wt% Y_2O_3-coated $LiNi_{0.5}Co_{0.2}Mn_{0.3}O_2$ are also improved significantly, especially at high rates (10C and 20C). X-ray diffraction (XRD) and X-ray photoelectron spectroscopy (XPS) are carried out to confirm the existence of Y_2O_3 layer on the $LiNi_{0.5}Co_{0.2}Mn_{0.3}O_2$ surface. Electrochemical impedance spectroscopy (EIS) and transmission electron microscopy (TEM) are applied to analyze the role of Y_2O_3-coating layer on the long cycling life and high rate capability.

1. Introduction

Recently, layered transition-metal oxide $LiNi_{0.5}Co_{0.2}Mn_{0.3}O_2$ as cathode material has been widely investigated due to its higher discharge capacity, lower cost and less toxicity than commercialized $LiCoO_2$ material [1–4]. However, its poor rate capability and severe capacity degradation at high operating voltage indeed limit its extensive application, especially at hybrid electric vehicles (HEVs) and energy storage systems [5]. One reason is that the electrode can easily react with the electrolyte at high voltage, which will destroy the surface of the active cathode materials and finally lead to the structure disruption and capacity fading dramatically [6]. Meanwhile, electrolytes used nowadays easily decompose at the surface of $LiNi_{0.5}Co_{0.2}Mn_{0.3}O_2$ especially at high operating voltage, which leads to an increase of interfacial impedance in the cell [7–10].

The surface coating has been proved to be an effective approach to improve the electrochemical performance of electrode materials. To date, metal oxides, fluorides, phosphates and other coating materials such as Li_2MnO_3 [11], Al_2O_3 [12], CuO [13], TiO_2 [14], AlF_3 [5], $FePO_4$ [15], SiP_2O_7 [16], TMSB [17] and Li_3VO_4 [18] have been coated on the surface of $LiNi_{0.5}Co_{0.2}Mn_{0.3}O_2$ to improve its electrochemical performance. According to the popular view, the metal oxides coating layer can isolate the bulk materials from the electrolyte, thus the material surface can be protected from electrolyte attack during the charge–discharge process. In recent years,

* Corresponding author. Department of Chemistry, School of Science, Tianjin University, People's Republic of China. Tel.: +86 22 27892379; fax: +86 22 27403475.
E-mail address: chenli_su@eyou.com (L. Chen).

http://dx.doi.org/10.1016/j.jpowsour.2014.05.047
0378-7753/

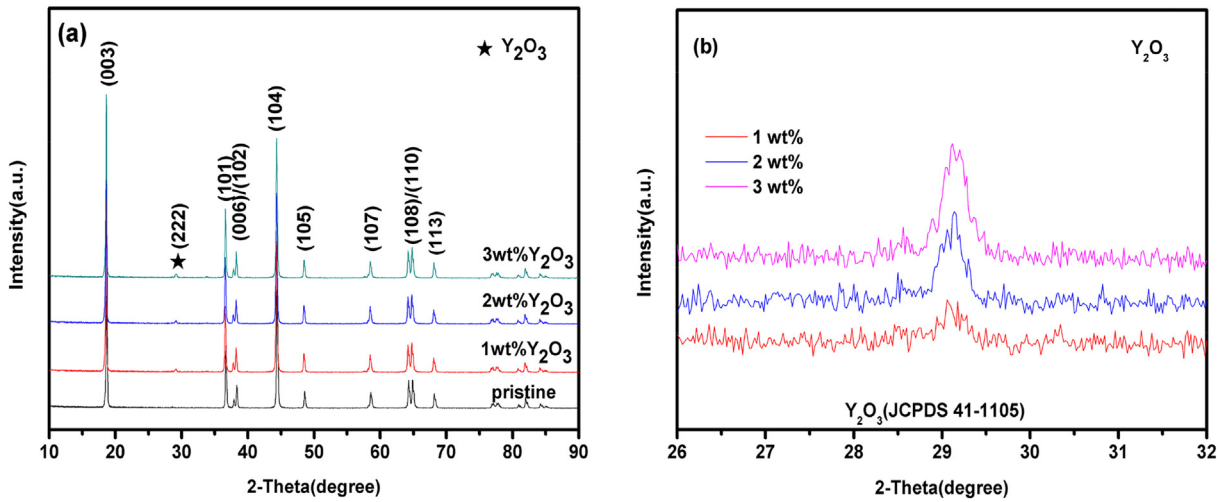

Fig. 1. XRD patterns of the bare and Y_2O_3-coated $LiNi_{0.5}Co_{0.2}Mn_{0.3}O_2$ powders with different coating amount.

yttrium oxide (Y_2O_3) not only has been used as various ceramics and luminescent materials because of its high corrosion resistance, outstanding thermostability and excellent chemical inertness [19], but also improves the electronic conductivity of yttrium-doped $SrTiO_3$ [20]. In addition, as rare-earth oxide, Y_2O_3 can form better electrical contact with the supported metal oxide to facilitate electron transfer [21,22]. Bai et al. [21] proposed that Y_2O_3 coating can block Mn dissolution from $LiMn_2O_4$ and improve its cycle stability at 2C. Wu et al. [22] reported that Y_2O_3 coating can effectively improve the cycling performance of $LiNi_{1/3}Co_{1/3}Mn_{1/3}O_2$ at lower rates (0.5C and 2C) between 2.8 and 4.5 V, but less studies on the rate capacity and the cycling performance at high cut-off voltage (>4.6 V) have been carried out. In this study, we investigate the effect of Y_2O_3 coating on high rate capability (10C and 20C) as well as the cycle stability at high operating voltages (4.6 V and 4.8 V) at room temperature.

2. Experimental

Commercially spherical $LiNi_{0.5}Co_{0.2}Mn_{0.3}O_2$ powder was utilized as the bare material. $Y(NO_3)_3 \cdot 6H_2O$ (reagent grade) used as raw material was dissolved in deionized water, then 5.0 g $LiNi_{0.5}Co_{0.2}Mn_{0.3}O_2$ powders were added into the $Y(NO_3)_3$ solution and stirred vigorously for 3 h at room temperature. The resulting mixture was heated at 60 °C under mechanical stirring to evaporate the solvent. Finally, the obtained precipitate was dried at 110 °C for 2 h and then calcined at 650 °C for 5.5 h to obtain Y_2O_3-coated $LiNi_{0.5}Co_{0.2}Mn_{0.3}O_2$ material.

The samples were characterized by Powder X-ray diffraction (XRD, D/max 2500 V/PC, Rigaku) using Cu-Kα radiation and a bent graphite monochromatic at 40 KV and 150 mA from 10° to 90° with a scanning rate of 2° min^{-1}. The morphology of the sample was examined by a transmission electron microscopy (TEM, JEM-2100F, JEOL) coupled with an energy-dispersive spectroscopy (EDS) at an accelerating voltage of 200 kV. The surface chemical composition of the powders were measured by X-ray photoelectron spectroscopy (XPS, AXIS Ultra DLD, Kratos) with a Al Kα line (1486.6 eV) as the X-ray source and operated in a vacuum of 10^{-9} Torr. The graphite peak at 284.6 eV was used as criterion for the final adjustment of the energy scale in the spectra. An aperture slot of 300 × 700 microns were used for all XPS spectra. Survey spectra and high resolution spectra were recorded with a pass energy of 160 eV and 40 eV respectively.

By mixing the active material, carbon black and polyvinylidene fluoride (PVDF) binder in a weight ratio of 8:1:1 in *N*-methyl-2 pyrrolidine (NMP) solvent, the cathode slurry was obtained and coated on aluminum foil, then it was dried at 120 °C for 12 h to get the electrode. The dried electrode was punched into round disks with a diameter of 1.2 cm and subsequently rolled into a thin film with a thickness of 32 μm. The electrolyte was 1 M $LiPF_6$ in ethylene

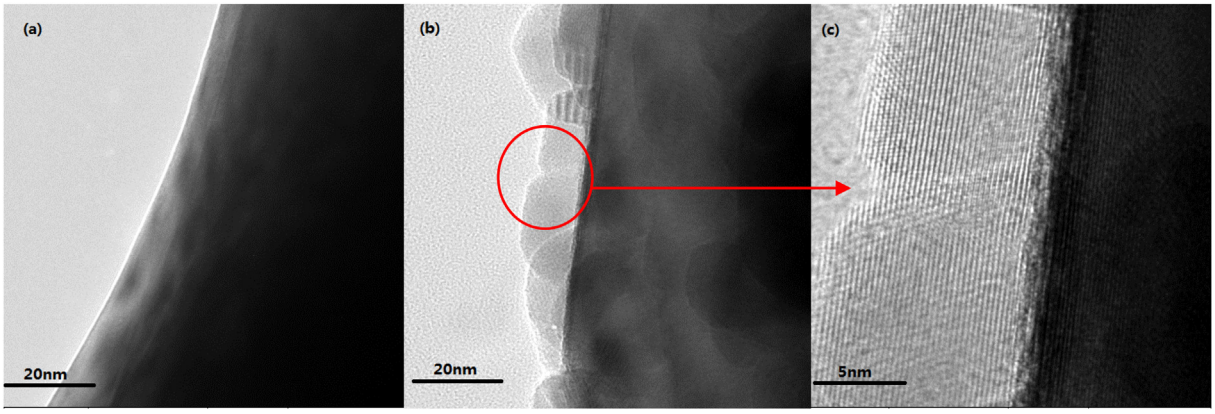

Fig. 2. TEM images of (a) bare and (b) 2 wt% Y_2O_3-coated $LiNi_{0.5}Co_{0.2}Mn_{0.3}O_2$; (c) magnified image of (b).

carbonate (EC)/ethyl methyl carbonate (EMC)/dimethyl carbonate (DEC) (1:1:1 by volume). The cells were assembled with the prepared cathodes and Li anodes in an argon-filled glove box where both the moisture and oxygen concentrations were maintained less than 1 ppm. The electrochemical properties of the cells were measured by a battery testing system (CT2001A, LAND) at rates from 1C to 20C (1C = 180 mA g^{-1}) at room temperature. Electrochemical impedance spectroscopy (EIS) were measured with an electrochemical workstation PARSTAT 2273 in the frequency range from 0.1 Hz to 100 kHz and a ±5 mV AC signal.

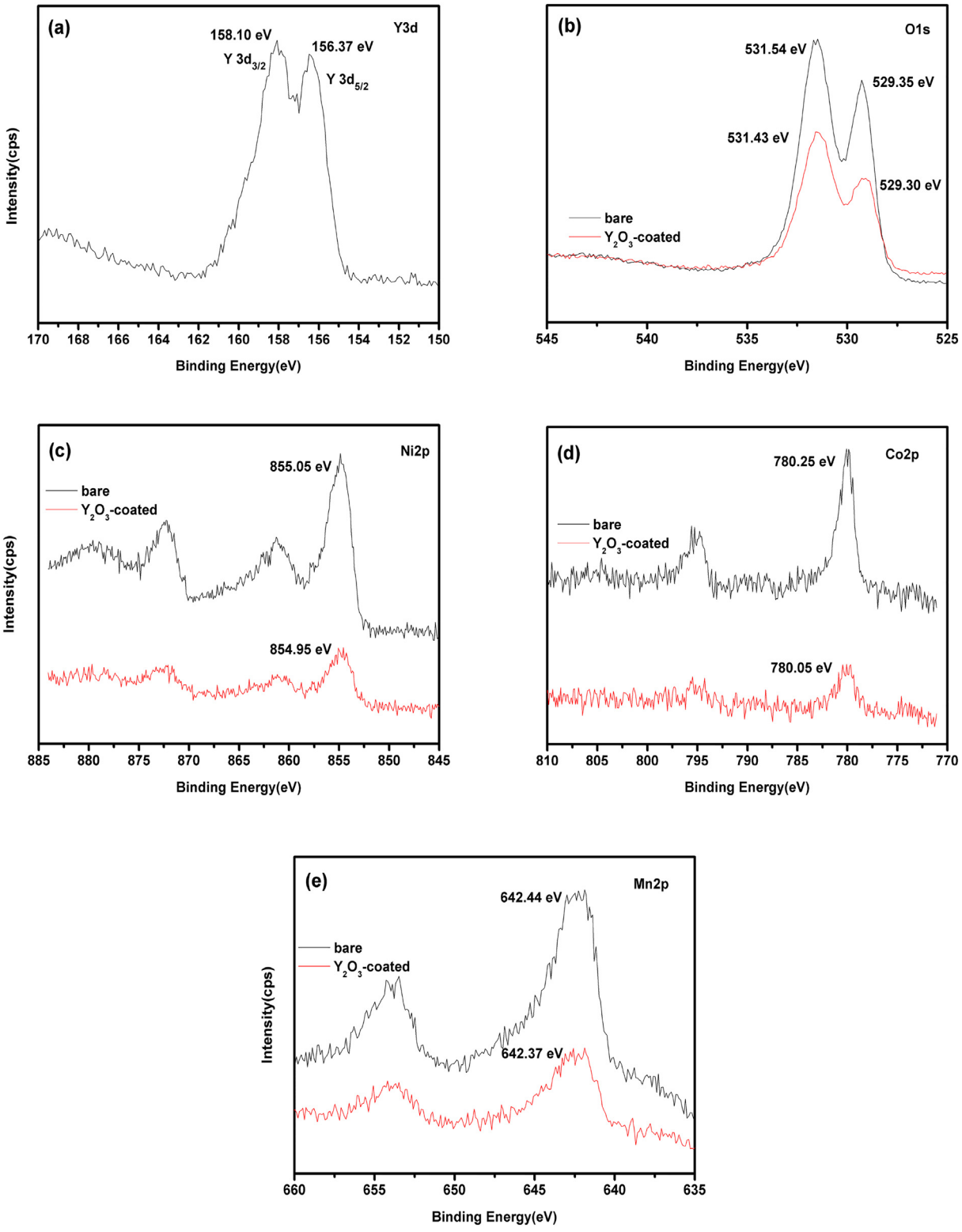

Fig. 3. XPS spectra of bare and 2 wt% Y_2O_3-coated $LiNi_{0.5}Co_{0.2}Mn_{0.3}O_2$. (a) Y3d; (b) O1s; (c) Ni2p; (d) Co2p and (e) Mn2p.

3. Results and discussion

The XRD patterns of the bare and Y_2O_3-coated $LiNi_{0.5}Co_{0.2}Mn_{0.3}O_2$ are presented in Fig. 1. All diffraction patterns can be indexed to a hexagonal α-$NaFeO_2$ structure with $R\bar{3}m$ group [23]. The distinct splitting of (006)/(102) and (108)/(110) peaks indicate the formation of a highly ordered layer structure. Besides the phase of $LiNi_{0.5}Co_{0.2}Mn_{0.3}O_2$, the XRD patterns for 2 wt% and 3 wt% Y_2O_3-coated samples in Fig. 1b present a second phase which corresponds to the crystalline phase of Y_2O_3 (JCPDS Card No. 41-1105), and the intensity of Y_2O_3 peak becomes stronger with the increase of Y_2O_3 amount. The peaks of $LiNi_{0.5}Co_{0.2}Mn_{0.3}O_2$ show no shift after Y_2O_3 coating, so the Y_2O_3 coating has no influence on the structure of the $LiNi_{0.5}Co_{0.2}Mn_{0.3}O_2$ bulk.

TEM images of the bare and 2 wt% Y_2O_3-coated $LiNi_{0.5}Co_{0.2}Mn_{0.3}O_2$ particles are given in Fig. 2. In contrast to the smooth surface of the bare (Fig. 2a), a coating layer can be observed on the surface of the Y_2O_3-coated $LiNi_{0.5}Co_{0.2}Mn_{0.3}O_2$ in Fig. 2b. The thickness of the Y_2O_3 coating layer is approximately 5–15 nm. Distinct crystal lattice of Y_2O_3 layer can be observed in Fig. 2c, which indicates that Y_2O_3 has well crystallinity.

Fig. 3shows the XPS spectra of the bare and 2 wt% Y_2O_3-coated $LiNi_{0.5}Co_{0.2}Mn_{0.3}O_2$. In Fig. 3a, the characteristic binding energies of Y $3d_{3/2}$ and Y $3d_{5/2}$ are 158.10 eV and 156.37 eV, respectively, which are in accordance with those of pure Y_2O_3 [24]. For Y_2O_3-coated $LiNi_{0.5}Co_{0.2}Mn_{0.3}O_2$, the peak at 531.43 eV in Fig. 3b corresponds to O1s which is bonded with Y^{3+} in Y_2O_3 [25], while the peak at 529.30 eV is considered to be O1s in the lattice of the bulk $LiNi_{0.5}Co_{0.2}Mn_{0.3}O_2$ [17]. For the spectrum of the bare sample in Fig. 3b, the peak at 529.35 eV belongs to O1s which is related with metal ions (Ni/Co/Mn), but the high peak at 531.54 eV is caused by the impurity Li_2CO_3 on the surface of $LiNi_{0.5}Co_{0.2}Mn_{0.3}O_2$ [26], and this peak disappears after coating Y_2O_3. Thus we can infer that the Y_2O_3 nanoparticles could inhibit the formation of impurities (such as Li_2CO_3) on the surface of $LiNi_{0.5}Co_{0.2}Mn_{0.3}O_2$, which may improve the electrochemical property of the electrode.

Compared to the bare $LiNi_{0.5}Co_{0.2}Mn_{0.3}O_2$, the Ni2p, Co2p and Mn2p peaks (in Fig. 3c–e) of Y_2O_3-coated $LiNi_{0.5}Co_{0.2}Mn_{0.3}O_2$ have no obvious chemical shift, indicating that the Ni, Co and Mn ion environments in the structure have not been changed. However, the intensities of the peaks all decrease obviously after coating, which is due to the formation of the Y_2O_3 layer on $LiNi_{0.5}Co_{0.2}Mn_{0.3}O_2$ surface.

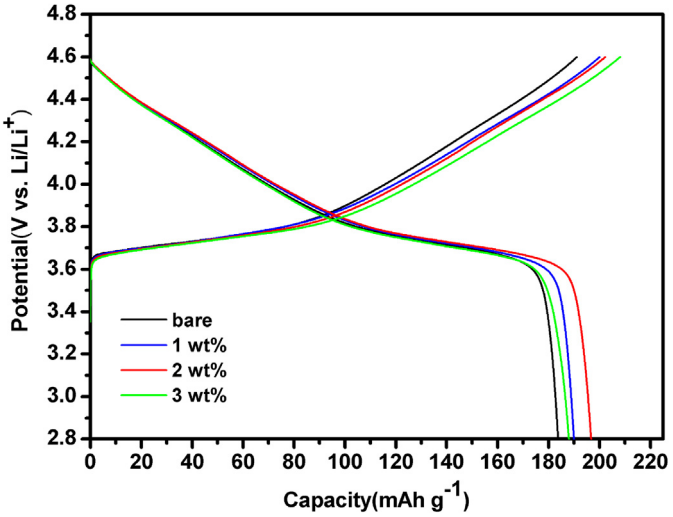

Fig. 4. The initial charge–discharge curves of bare and Y_2O_3-coated $LiNi_{0.5}Co_{0.2}Mn_{0.3}O_2$ at 0.1C between 2.8 and 4.6 V.

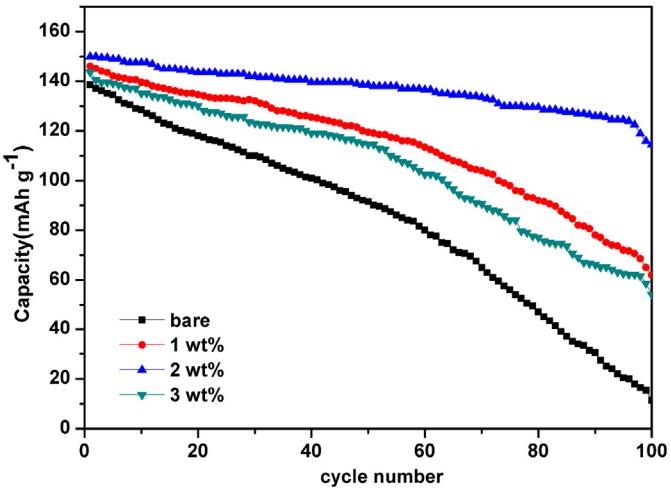

Fig. 5. Cycle performance of bare and Y_2O_3-coated $LiNi_{0.5}Co_{0.2}Mn_{0.3}O_2$ electrodes at 10C in the voltage range of 2.8–4.6 V.

Fig. 4shows the initial charge–discharge curves of the bare and Y_2O_3-coated $LiNi_{0.5}Co_{0.2}Mn_{0.3}O_2$ at 0.1C (18 mA g^{-1}) between 2.8 and 4.6 V. All the charge–discharge curves show the typical potential plateaus of layered $LiNi_{0.5}Co_{0.2}Mn_{0.3}O_2$ at 3.75 V, which is related to the Ni^{2+}/Ni^{4+} redox couple [27]. But for the Y_2O_3-coated samples, their potentials obviously increase more slowly at the end of charge process than that of the bare one, which indicates that Y_2O_3 coating can reduce polarization to some extent [28]. The main reason for the improvement is that Y_2O_3 layer can effectively enhance the electronic conductivity of the cathode [14,28] and facilitate Li^+ diffusion at the electrode/electrolyte interface [29]. As shown in Fig. 4, the bare $LiNi_{0.5}Co_{0.2}Mn_{0.3}O_2$ delivers a discharge capacity of 183.7 mAh g^{-1}, and all the Y_2O_3-coated samples exhibit higher initial discharge capacities than the bare sample, which are 190.0, 196.7 and 188.0 mAh g^{-1} for 1 wt%, 2 wt% and 3 wt% Y_2O_3-coated samples in sequence.

The cycle performances of all samples, in the voltage range of 2.8–4.6 V at 10C, are given in Fig. 5. The cells were charged at 1C and discharged at 10C. All the coated samples exhibit higher discharge capacities and capacity retentions than the bare one, and the 2 wt% Y_2O_3-coated sample exhibits the longest cycle life. The

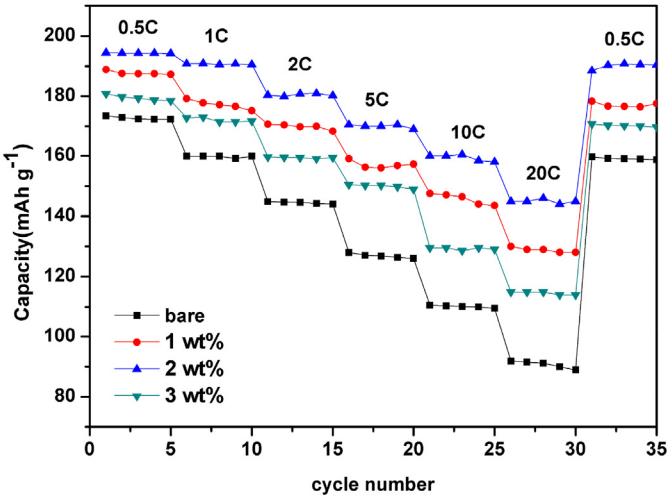

Fig. 6. Rate capacity of the bare and Y_2O_3-coated $LiNi_{0.5}Co_{0.2}Mn_{0.3}O_2$ from 0.05C to 20C between 2.8 and 4.6 V.

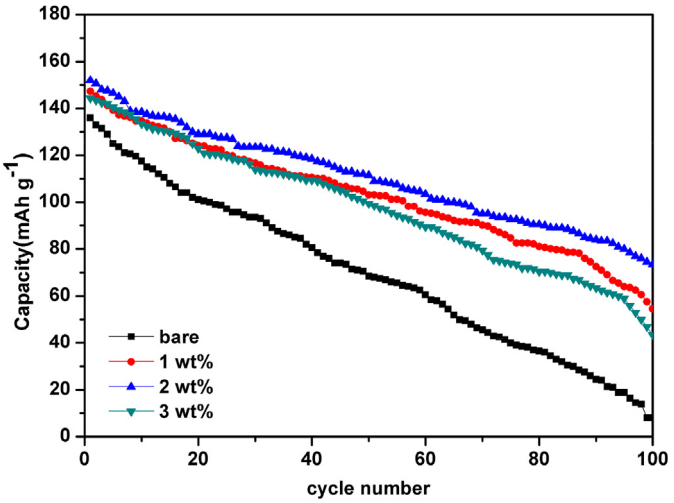

Fig. 7. Cycling performance of bare and Y_2O_3-coated $LiNi_{0.5}Co_{0.2}Mn_{0.3}O_2$ at 10C in the voltage range of 2.8–4.8 V.

discharge capacity of the bare $LiNi_{0.5}Co_{0.2}Mn_{0.3}O_2$ decreases sharply from 138.5 to 11.5 mAh g^{-1} after 100 cycles, only 8.3% discharge capacity left. For the 2 wt% Y_2O_3-coated sample, it can deliver a higher initial capacity of 150.0 mAh g^{-1}, and still remains a discharge capacity of 114.5 mAh g^{-1} with a much higher capacity retention of 76.3% after 100 cycles. The capacity retentions of 1 wt% and 3 wt% Y_2O_3-coated samples are 41.1% and 37.6%, respectively. The excellent capacity retention of 2 wt% Y_2O_3-coated sample at high current density can be attributed to the appropriate coating amount of Y_2O_3. Y_2O_3 can enhance the electronic conductivity of the cathode, but conversely an excess Y_2O_3 layer may hinder the diffusion of Li^+ and result in the low Li^+ diffusion coefficient (D_{Li+}) [30–32], which can be proved by the following EIS test. Taking into account both electronic conductivity and Li^+ diffusion, an optimum Y_2O_3 coating amount should exist [32].

The rate capabilities of the bare and Y_2O_3-coated samples are further investigated in Fig. 6. The cells are charged to 4.6 V at 1C, and discharged to 2.8 V at 0.5C, 1C, 2C, 5C, 10C and 20C, respectively, then cycled at 0.5C again, and the test at each rate sustains for five cycles. With the discharge current density increasing, the discharge capacities of all the samples decrease due to polarization [29]. While the Y_2O_3-coated samples exhibit noticeably better rate performance than that of the bare sample at any rate, especially at high rates (10C and 20C). The 2 wt% Y_2O_3-coated sample can deliver 160.5 mAh g^{-1} at 10C and 145.9 mAh g^{-1} at 20C, which respectively are 82.7% and 75.2% of the initial capacity at 0.5C. While the bare $LiNi_{0.5}Co_{0.2}Mn_{0.3}O_2$ can deliver only 109.5 mAh g^{-1} at 10C and 88.9 mAh g^{-1} at 20C, whose capacities retention are only 63.1% and 51.2% of its initial capacity at 0.5C (173.4 mAh g^{-1}), respectively. When cycled at 0.5C again, 2 wt% Y_2O_3-coated sample shows a capacity recovery of 98.0%, which is higher than that of the bare one (91.1%). This result indicates that the Y_2O_3-coating layer improves the reversibility of Li^+ diffusion at the electrode/electrolyte interface in intercalation/deintercalation process [22].

Compared with those of $LiNi_{0.5}Co_{0.2}Mn_{0.3}O_2$ coated with TiO_2 [14] and AlF_3 [5], the rate capabilities of Y_2O_3-coated samples are much better. So we speculate that Y_2O_3 not only enhances the electronic conductivity of the cathode surface, but also forms better electrical contact with the $LiNi_{0.5}Co_{0.2}Mn_{0.3}O_2$ bulk to facilitate electron transfer [22].

The discharge capacities and cycling performances of the bare and Y_2O_3-coated samples in the voltage range of 2.8–4.8 V are

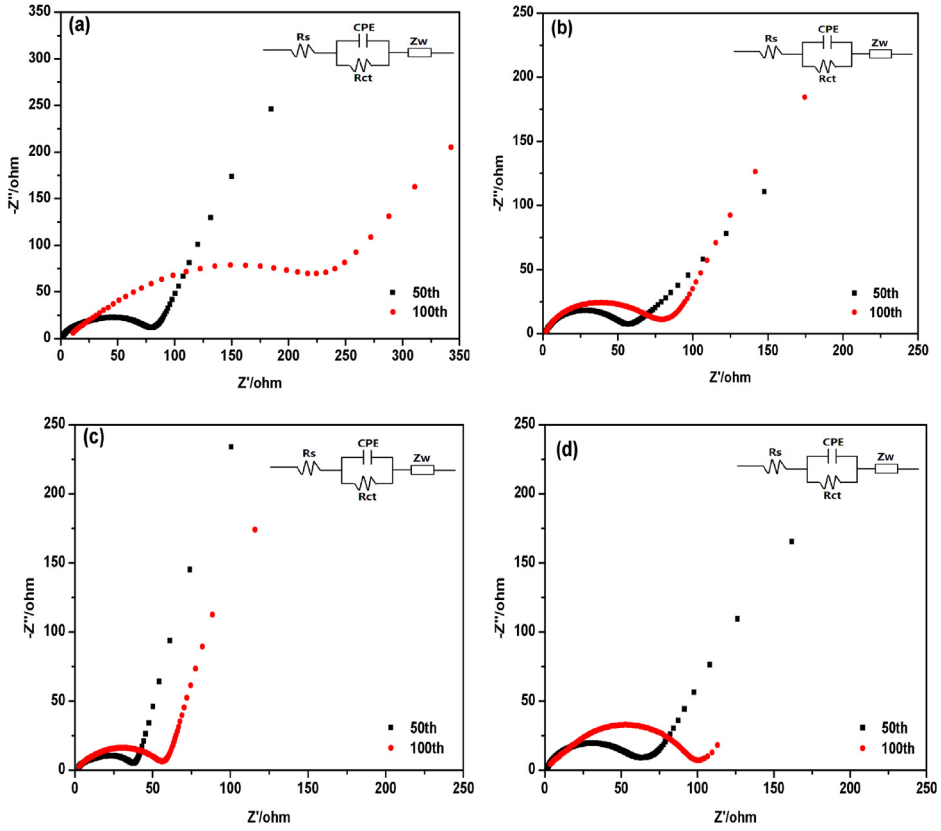

Fig. 8. The EIS plots of bare (a) and 1, 2, 3 wt% Y_2O_3-coated $LiNi_{0.5}Co_{0.2}Mn_{0.3}O_2$ (b, c, d).

Table 1
The values of R_{ct} and D_{Li+} at different number of cycles.

Samples	R_{ct} (Ω)		D_{Li+}($cm^2\ s^{-1}$)	
Cycle number	50th	100th	50th	100th
Bare	80.5	260.0	8.99×10^{-13}	5.83×10^{-13}
1 wt% Y_2O_3-coated	65.0	75.2	5.02×10^{-12}	2.32×10^{-12}
2 wt% Y_2O_3-coated	34.4	56.5	8.84×10^{-12}	3.10×10^{-12}
3 wt% Y_2O_3-coated	70.0	102.0	4.26×10^{-12}	1.80×10^{-12}

shown in Fig. 7. The cells were charged at 1C and discharged at 10C. After 100 cycles, the discharge capacities of the bare sample as well as 1 wt%, 2 wt% and 3 wt% Y_2O_3-coated samples are 8.0, 54.6, 74.5 and 43.5 mAh g^{-1}, respectively, and the sequential capacity retentions are 5.9%, 37.0%, 49.0% and 30.1%. Apparently, the cycle performance, even at high discharge rate (10C) and high cut-off voltage (4.8 V), is still improved by Y_2O_3 coating. But it is worth noting that the discharge capacities and capacity retentions at 4.8 V for all samples, especially for the bare sample, are less than those at 4.6 V under the same discharge rate, which is attributed to the acceleration of the side reaction between electrode and electrolyte at 4.8 V. Thus, Y_2O_3 coating layer still plays an important role in alleviating the side reaction between $LiNi_{0.5}Co_{0.2}Mn_{0.3}O_2$ and electrolyte at high cut-off voltage, and further stabilizing the structure of $LiNi_{0.5}Co_{0.2}Mn_{0.3}O_2$ in the high voltage region at a certain degree.

The Nyquist plots of the bare and coated samples at 10C between 2.8 and 4.8 V (after 50 and 100 cycles) are presented in Fig. 8. All EIS plots consist of a depressed semicircle in the high to medium frequency and a quasi-straight line in the low frequency. The semicircle is assigned to the interfacial charge transfer resistance (R_{ct}), and the slope line is related to Warburg impedance (W), which is associated with Li^+ diffusion in the powder particles [33].

R_{ct} is obtained by fitting ZSimpWin software [18]. As shown in Fig. 8a, the R_{ct} value of the bare $LiNi_{0.5}Co_{0.2}Mn_{0.3}O_2$ is much higher than those of Y_2O_3-coated samples after long term cycling. For the bare $LiNi_{0.5}Co_{0.2}Mn_{0.3}O_2$, the R_{ct} value increases drastically from 80.5 Ω (50th cycle) to 260.0 Ω (100th cycle), which certainly leads to a poor rate capacity. However, the R_{ct} values of all Y_2O_3-coated samples increase more slowly during cycling, especially for the 2 wt % Y_2O_3-coated sample whose R_{ct} value is only 56.5 Ω after 100 cycles, about one-fourth of that for the bare sample. D_{Li+} is calculated according to the equation reported by Huo et al. [34]. The R_{ct} values and D_{Li+} values are listed in Table 1. Obviously, the D_{Li+} of Y_2O_3-coated samples decrease less than that of the bare sample. The D_{Li+} of 2 wt% Y_2O_3-coated sample is 3.10×10^{-12} $cm^2\ s^{-1}$ after 100 cycles, which is about 5 times larger than that of the bare one (5.83×10^{-13} $cm^2\ s^{-1}$). This result indicates that Y_2O_3 layer facilitates the diffusion of Li^+ at the interface of electrode and electrolyte. Usually, the rate performance of the electrode material strongly depends on both the charge transfer process and Li^+ diffusion process. Thus, the excellent rate performance of 2 wt% Y_2O_3-coated sample can be attributed to the smallest R_{ct} and the largest D_{Li+}.

TEM images of the bare and 2 wt% Y_2O_3-coated $LiNi_{0.5}Co_{0.2}Mn_{0.3}O_2$ after 100 cycles at 10C between 2.8 and 4.8 V are shown in Fig. 9. Obviously, the smooth surface of the bare sample (Fig. 2a) has become rough (Fig. 9a), which indicates that the surface

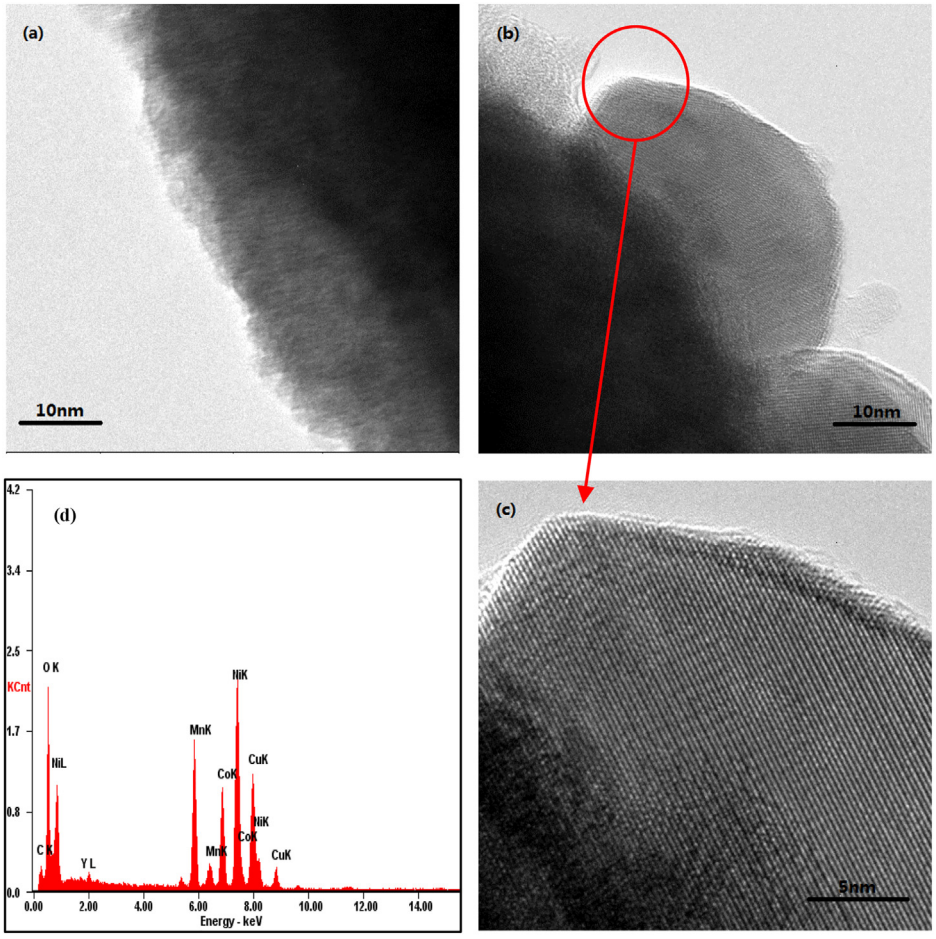

Fig. 9. TEM images of (a) bare and (b) 2 wt% Y_2O_3-coated $LiNi_{0.5}Co_{0.2}Mn_{0.3}O_2$ after 100 cycles; (c) magnified image of (b); (d) EDS spectra of 2 wt% Y_2O_3-coated $LiNi_{0.5}Co_{0.2}Mn_{0.3}O_2$.

of the bare sample has been damaged after cycling [35,36]. While for 2 wt% Y_2O_3-coated $LiNi_{0.5}Co_{0.2}Mn_{0.3}O_2$, the Y_2O_3 layer with well crystallinity can still tightly fasten on the $LiNi_{0.5}Co_{0.2}Mn_{0.3}O_2$ surface, which indicates that the structure of Y_2O_3 is still stable even after long-term cycling. In addition, EDS spectra of 2 wt% Y_2O_3-coated $LiNi_{0.5}Co_{0.2}Mn_{0.3}O_2$ in Fig. 9d also confirms the existence of Y. Thus we can infer that Y_2O_3 coating layer can effectively protect the surface of the bulk $LiNi_{0.5}Co_{0.2}Mn_{0.3}O_2$ from electrolyte attack. So the stable existence of Y_2O_3 on $LiNi_{0.5}Co_{0.2}Mn_{0.3}O_2$ surface is beneficial to the long cycle performance of $LiNi_{0.5}Co_{0.2}Mn_{0.3}O_2$ at high cut-off voltage. As a result, the 2 wt% Y_2O_3-coated sample shows an outstanding electrochemical performance.

4. Conclusions

Y_2O_3 coated $LiNi_{0.5}Co_{0.2}Mn_{0.3}O_2$ shows excellent electrochemical performance, especially the outstanding high capacity and cycling stability at high discharge rate under different high cut-off voltages. The 2 wt% Y_2O_3-coated $LiNi_{0.5}Co_{0.2}Mn_{0.3}O_2$ shows a much higher capacity retention of 76.3% than that of the bare one (8.3%) after 100 cycles at 10C between 2.8 and 4.6 V, and it also exhibits the best electrochemical property at 10C and at a higher voltage of 4.8 V. The improved electrochemical performance of Y_2O_3-coated $LiNi_{0.5}Co_{0.2}Mn_{0.3}O_2$ can be attributed to the stable Y_2O_3 layer with well crystalline which can protect $LiNi_{0.5}Co_{0.2}Mn_{0.3}O_2$ from electrolyte attack and improve the charge transfer and Li^+ diffusion ability. So Y_2O_3 coating is an effective method to solve the existing problems (poor rate capability and capacity retention at high voltage) of layer $LiNi_{0.5}Co_{0.2}Mn_{0.3}O_2$ material for the practical application in hybrid electric vehicles and energy storage systems.

Acknowledgment

The authors acknowledge the financial support of Tianjin Huaxia Hongyuan industrial Co., Ltd.

References

[1] Z. Liu, A. Yu, J.Y. Lee, J. Power Sources 81-82 (1999) 416–419.
[2] M.-H. Kim, H.-S. Shin, D. Shin, Y.-K. Sun, J. Power Sources 159 (2006) 1328–1333.
[3] L.-J. Li, X.-H. Li, Z.-X. Wang, H.-J. Guo, P. Yue, W. Chen, L. Wu, J. Alloys Compd. 507 (2010) 172–177.
[4] P. He, H. Yu, D. Li, H. Zhou, J. Mater. Chem. 22 (2012) 3680.
[5] K. Yang, L.-Z. Fan, J. Guo, X.H. Qu, Electrochim. Acta 63 (2012) 363–368.
[6] J.G. Li, L. Wang, Q. Zhang, X.M. He, J. Power Sources 190 (2009) 149–153.
[7] D. Aurbach, K. Gamolsky, B. Markovsky, G. Salitra, Y. Gofer, U. Heider, R. Oesten, M. Schmidt, J. Electrochem. Soc. 147 (2000) 1322.
[8] D. Ostrovskii, F. Ronci, B. Scrosati, P. Jacobsson, J. Power Sources 94 (2001) 183.
[9] D. Ostrovskii, F. Ronci, B. Scrosati, P. Jacobsson, J. Power Sources 103 (2001) 10.
[10] P. Arora, R.E. White, J. Electrochem. Soc. 145 (1998) 3647.
[11] X.K. Yang, X.Y. Wang, L. Hu, G.S. Zou, S.J. Su, Y.S. Bai, H.B. Shu, Q.L. Wei, B. Hu, L. Ge, D. Wang, L. Liu, J. Power Sources 242 (2013) 589–596.
[12] K.J. Cao, L. Wang, L. Li, G.C. Liang, Appl. Mech. Mater. 320 (2013) 235–240.
[13] T. Liu, S.-X. Zhao, K.Z. Wang, C.-W. Nan, Electrochim. Acta 85 (2012) 605–611.
[14] W. Liu, M. Wang, X.L. Gao, W.D. Zhang, J.T. Chen, H.H. Zhou, X.X. Zhang, J. Alloys Compd. 543 (2012) 181–188.
[15] Y.S. Bai, X.Y. Wang, S.Y. Yang, X.Y. Zhang, X.K. Yang, H.B. Shu, Q. Wu, J. Alloys Compd. 541 (2012) 125–131.
[16] Y.-S. Lee, D. Ahn, Y.-H. Cho, T.E. Hong, J. Cho, J. Electrochem. Sco 158 (2011) A1354–A1360.
[17] X.X. Zuo, C.J. Fan, J.S. Liu, X. Xiao, J.H. Wu, J.M. Nan, J. Power Sources 229 (2013) 308–312.
[18] Y. Huang, F.-M. Jin, F.-J. Chen, L. Chen, J. Power Sources 256 (2014) 1–7.
[19] B.W. Ju, X.Y. Wang, C. Wu, Q.L. Wei, X.K. Yang, H.B. Shu, Y.S. Bai, J. Solid State Electrochem. 18 (2014) 114–123.
[20] S.Q. Hui, A. Petric, Mater. Res. Bull. 37 (2002) 1215–1231.
[21] Y. Bai, F. Wu, H.-T. Yang, Y. Zhong, C. Wu, Adv. Mater. Res. 391-392 (2012) 1069–1074.
[22] F. Wu, M. Wang, Y.F. Su, S. Chen, J. Power Sources 189 (2009) 743–747.
[23] Z.H. Lu, L.Y. Beaulieu, R.A. Donaberger, C.L. Thomas, J.R. Dahn, J. Electrochem. Soc. 149 (2002) A778–A791.
[24] J. Cho, C.-S. Kim, S.-I. Yoo, Electrochem. Solid-State Lett. 3 (2000) 265–362.
[25] H. Pedersen, F. Soderlind, R.M. Petoral, K. Uvdal, P.-O. Kall, L. Ojamae, Surf. Sci. 592 (2005) 124–140.
[26] D.P. Abraham, R.D. Twesten, M. Balasubramanian, I. Petrov, J. McBreen, K. Amine, Electrochem. Commun. 4 (2002) 620–625.
[27] J.R. Dahn, U. von Sacken, C.A. Michal, Solid State Ionics 44 (1990) 87–97.
[28] F. Wu, M. Wang, Y.F. Su, S. Chen, B. Xu, J. Power Sources 191 (2009) 628–632.
[29] X.Z. Liu, H.Q. Li, D. Li, M. Ishida, H.S. Zhou, J. Power Sources 243 (2013) 374–380.
[30] B.W. Ju, X.Y. Wang, C. Wu, Q.L. Wei, X.K. Yang, H.B. Shu, Y.S. Bai, J. Solid State Electrochem. 18 (2014) 115–123.
[31] Y.P. Chen, Y. Zhang, B.J. Chen, Z.Y. Wang, C. Lu, J. Power Sources 256 (2014) 20–27.
[32] X.H. Rui, C. Li, C.H. Chen, Electrochim. Acta 54 (2009) 3374–3380.
[33] D. Wang, Y. Huang, Z.Q. Huo, L. Chen, Electrochim. Acta 107 (2013) 461–466.
[34] Z.-Q. Huo, Y.-T. Cui, D. Wang, Y. Dong, L. Chen, J. Power Sources 245 (2014) 331–336.
[35] P. Yue, Z.X. Wang, H.J. Guo, X.H. Xiong, X.H. Li, Electrochim. Acta 92 (2013) 1–8.
[36] Y.-K. Sun, C.S. Yoon, C.K. Kim, S.G. Youn, Y.-S. Lee, M. Yoshio, I.-H. Oh, J. Mater. Chem. 11 (2001) 2519–2522.